

Aerosol Characterization Based on Graphical Method of Gobbi Diagrams

KOUTOUNIDIS I.*, GIANNAKAKI E.

Department of Environmental Physics and Meteorology, Faculty of Physics, University of Athens, 15784 Athens, Greece

*corresponding author: Koutounidis Ioannis

e-mail: giannis.koutounidis@gmail.com

Abstract A practical graphical approach for translating \AA and its spectral curvature ($\Delta\text{\AA}$) into estimates of fine-mode aerosol radius and its contribution to total AOT was proposed by Gobbi et al. (2007). In the present study, we utilize AERONET Version 3 Level 3 data—specifically lidar ratio and depolarization ratio products—to evaluate the potential of this graphical method for aerosol type classification.

Keywords: AERONET, aerosol type, Gobbi diagram

1. Introduction

Atmospheric aerosols play a key role in influencing the Earth's climate through direct, indirect, and semi-direct effects. However, accurately quantifying these impacts is challenging due to the significant temporal and spatial variability in aerosol concentration and their associated physical, optical, and chemical properties.

The Ångström exponent (\AA), derived from the spectral dependence of aerosol optical thickness (AOT), is widely used as an indicator of the dominant particle size in the atmospheric column. Values of $\text{\AA} \leq 1$ generally indicate a prevalence of coarse-mode aerosols (radii $\geq 0.5 \mu\text{m}$), such as mineral dust and sea salt, while values of $\text{\AA} \geq 1.5$ suggest dominance by fine-mode aerosols (radii $< 0.5 \mu\text{m}$), commonly associated with urban pollution and biomass burning. Schuster et al. (2006) emphasized the importance of the selected wavelength pair in calculating \AA , as this influences the sensitivity of the metric. Specifically, \AA values derived from longer wavelength pairs (e.g., 670–870 nm) are sensitive to the fine-mode fraction, while those from shorter wavelengths (e.g., 380–440 nm) are more responsive to the fine-mode effective radius.

Nevertheless, the Ångström exponent alone cannot distinguish the relative contributions of fine- and coarse-mode aerosols in mixed aerosol conditions. For instance, large fine-mode particles can yield the same \AA as a combination of small fine- and coarse-mode particles (Gobbi et al., 2007). To address this limitation, several studies have explored how the spectral variation of \AA can provide further insight into aerosol size distribution (Schuster et al., 2006). Kaufman (1993) proposed that a negative difference in Ångström exponent—defined as $\Delta\text{\AA} = \text{\AA}(440 \text{ nm}, 613 \text{ nm}) - \text{\AA}(440 \text{ nm}, 1003 \text{ nm})$ —indicates dominance by fine-mode aerosols, whereas a positive $\Delta\text{\AA}$

points to a bimodal distribution with a significant coarse-mode component.

2. Methodology

Considering the operating wavelengths of AERONET sun photometers, \AA was derived for the wavelength pairs of 440–870 nm, and its spectral curvature was represented by the difference $\Delta\text{\AA} = \text{\AA}(440, 675) - \text{\AA}(675, 870)$. The version 3 inversion products were also used that provide the spectral particle linear depolarization ratios and lidar ratios.

Firstly, the data were divided in classes of different AOT (intervals of 0.05). The different AOTs occupy different parts of the plot, indicating that the same Aerosol Optical Depth could be the result of different aerosol size and different fraction of fine to coarse aerosols. Thus, we used clusters of single scattering albedo of 0.1 intervals for the graphical display.

Eight AERONET stations were included in the analysis, with the Thessaloniki site selected for demonstration purposes.

3. Results

In the initial analysis, the data were categorized based on different aerosol optical thickness (AOT) classes. Color coding was applied to intervals of 0.05 AOT (Figure 1, top). The resulting distribution showed that different AOT values occupied distinct regions of the plot. This suggests that similar AOT values can result from varying aerosol size distributions and different fine-to-coarse aerosol fractions.

To better capture this variability, a second classification was performed using intervals of 0.1 in single-scattering albedo (SSA). In this case, the graphical representation showed a clearer clustering, where specific color intervals occupied well-defined areas. This indicates that lower SSA values are associated with a reduced contribution of fine particles to the total optical depth.

A third classification was then conducted using the lidar ratio, divided into 10 sr intervals. However, in this case, the color-coded intervals did not consistently occupy

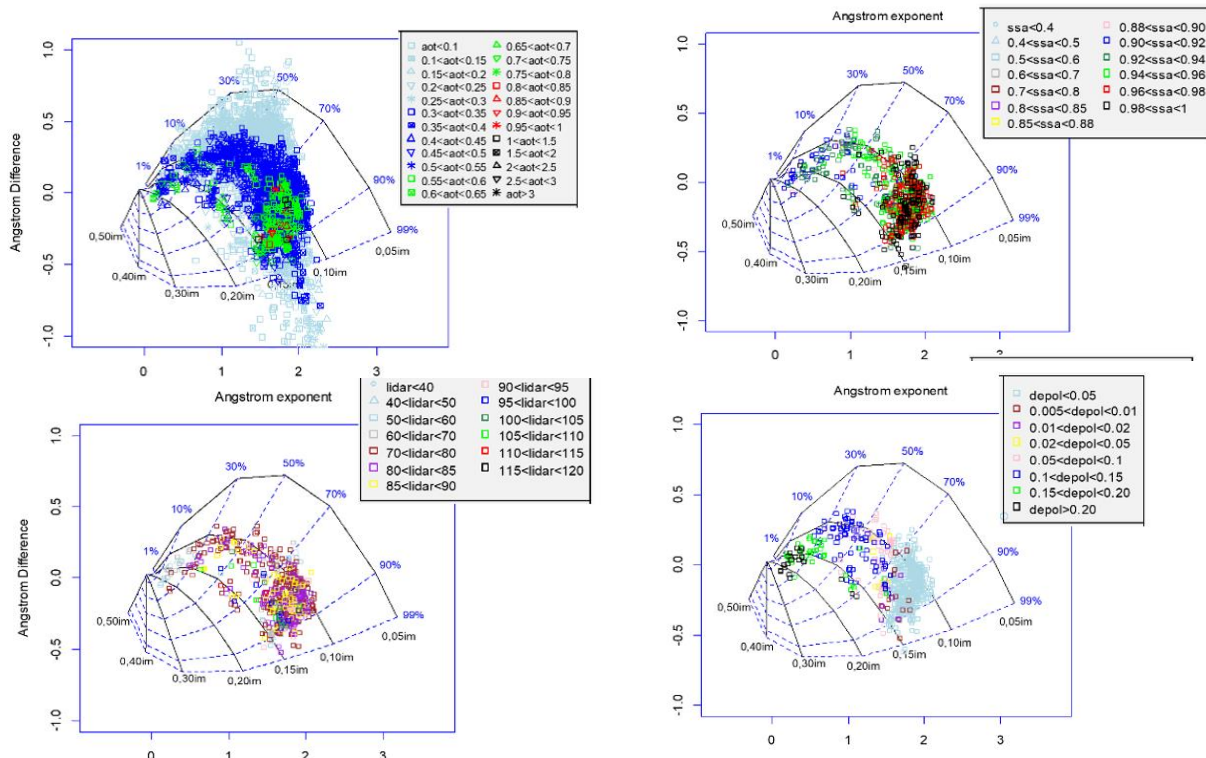
distinct areas of the plot. This suggests that the lidar ratio is not directly correlated with the fine particle contribution to the total optical depth.

In the fourth and final classification, the data were grouped according to depolarization ratio intervals. This approach revealed a clear relationship: as the depolarization ratio increases—indicating more irregular, non-spherical particles—the contribution of fine particles to the total optical depth decreases. However, the fine particles that do contribute tend to be larger.

We found that the smaller the single scattering albedo the lower the percentage that fine particles contributes to the total optical depth. In the third attempt the classification

of 10 sr. The contribution of fine particles to the total optical depth is not directly correlated to the lidar ratio parameter. Lastly, we used different intervals of the depolarization ratio parameter. It is clear that the contribution of fine particles to the total optical depth is directly correlated with different values of depolarization values. The more unspherical the particles the larger the depolarization ratio and the lower the contribution of fine particles to the total optical depth but with larger fine particles.

Future work will involve expanding this analysis to include both pure and mixed AERONET stations equipped with lidar-depolarization measurement capabilities, enabling a broader and more detailed understanding of aerosol



was performed using the lidar ratio parameter in intervals

characteristics.

Figure 1. Gobi graphical display of Thessaloniki AERONET data for different classes of Aerosol optical thickness, single scattering albedo, lidar ratio and depolarization ratio

Acknowledgements

The research work was supported by the Hellenic Foundation for Research and Innovation (H.F.R.I.) under the “Basic Research Financing (Horizontal support for all Sciences), National Recovery and Resilience Plan (Greece 2.0)” (Project Acronym: SCOPE, Project Number: 015144)

References

- Dubovik, O., et al. (2006). Application of spheroid models to account for aerosol particle nonsphericity in remote sensing of desert dust. *Journal of Geophysical Research: Atmospheres*, **111**.
- Gobbi, G. P., et al. (2007). Classification of aerosol properties derived from AERONET direct sun data. *Atmospheric Chemistry and Physics*, **7**(2), 453-458.

- Kaufman, Y. J. (1993). Aerosol optical thickness and atmospheric path radiance. *Journal of Geophysical Research: Atmospheres*, **98**, 2677-2692.

- Schuster, G. L., et al. (2006). Angstrom exponent and bimodal aerosol size distributions. *Journal of Geophysical Research: Atmospheres*, **111**.